Tannic acid inhibits electrogenic Na+/HCO3– co-transporter activity in embryonic neural stem cell-derived radial glial-like cells

Tommy Nordström[a], Gao Zhenyu[b], Leif C. Andersson[c] and Karl E.O. Åkerman[a]

Self-renewing neural stem cells and progenitor cells are cell populations that generate radial glial cells and neurons through asymmetric division. Regulation of intracellular pH in stem cells with high metabolic activity is critical for both cell signaling and proliferation. We have recently found that a S0859-inhibitable electrogenic Na^+/HCO_3^- co-transporter (NBCe1, Slc4a4), is the primary pH_i regulatory mechanism in stem cell-derived radial glial-like cells. Here we show, by using the voltage-sensitive fluorescent dye $DiBAC_4(3)$ and BCECF, a pH-sensitive dye, that an antioxidant, tannic acid (100 µM), can inhibit potassium- and calcium-dependent rapid changes in membrane potential and NBCe1 mediated pH_i regulation in brain-derived glial-like cells *in vitro*. Furthermore, neural stem cell differentiation and neurosphere formation (proliferation) were completely inhibited by tannic acid. The present study provides evidence that tannic acid is a natural inhibitor of NBCe1. It is tempting to speculate that tannic acid or related compounds that inhibits NBCe1-mediated pHi regulation in glial-like cells may also have bearing on the treatment of glial neoplasms. *NeuroReport* 31: 57–63 Copyright © 2019 The Author(s). Published by Wolters Kluwer Health, Inc.

NeuroReport 2020, **31**:57–63

Keywords: calcium, hyperpolarization, Na+/HCO3– co-transporter, NBCe1, pH, stem cell, tannic acid

[a]Faculty of Medicine, Medicum, Division of Physiology, University of Helsinki, Helsinki, Finland, [b]School of Pharmacy, Suzhou Vocational Health College, Suzhou, Jiangsu, China and [c]Department of Pathology, University of Helsinki, Helsinki, Finland

Correspondence to Tommy Nordström, PhD, Faculty of Medicine, Medicum, Division of Physiology, P.O. Box 63, University of Helsinki, FIN-00014 Helsinki, Finland
Tel: +358 504482151; e-mail: tommy.nordstrom@helsinki.fi

Received 19 September 2019 **Accepted** 15 October 2019

Introduction

Tannins represent a large family of water-soluble phenolic compounds that are present in many plants. Non-hydrolysable condensed tannins (proanthocyanidins) and hydrolysable tannins like tannic acid (TA) are known to have strong antioxidant properties [1]. The antioxidant properties are due to the fact that they can bind redox active metals such as iron and copper and thereby inhibit the formation of reactive oxygen species (free radicals) through the Fenton reaction [2–4].

During the past decade, it has been shown that TA can inhibit proliferation and migration of prostate and colon cancer cells [5,6]. Moreover, TA has been reported to affect cell cycle progression and induce G1 arrest in squamous cell carcinoma, breast cancer and leukemic T cells [7] and to induce apoptosis in prostate and glioma cell lines [8–10]. TA has also been shown to protect brain tissue during ischemia [11] and protect brain tissue exposed to heavy metals [12].

In some reports, specific intracellular signaling steps (involving kinases and transcription factors) have been shown to be affected by TA [13–16]. However, to these reported intracellular effects, TA has also been shown to interfere with a variety of anion and cation channels in the cell membrane. A calcium-sensitive chloride channel TME16A can efficiently be blocked by TA [17–19]. Effects on potassium channels hERG and Kv channels [20,21] and L-type calcium channels have also been reported [22].

Here we have studied the effects of TA on the electrogenic Na^+/HCO_3^- co-transporter (NBCe1), which is the primary pH_i regulatory mechanism in stem cell-derived glial-like cells [23]. Our results show that TA has strong impact on NBCe1 mediated pH_i regulation in glial-like cells. The scenario that TA depresses cell proliferation and progression through the cell cycle by inhibiting NBCe1 mediated pH_i regulation is discussed.

Materials and methods

Cell culture

Neural progenitor cells (NPCs) were generated as previously described [24]. Cells were scraped from the anterior portion of the lateral wall of the lateral ventricles of E14 embryonic mouse brains. The cells were grown as free-floating aggregates termed neurospheres. Dissociated cells were plated in DMEM/F-12 'complete' culture medium (Gibco, Life Technologies) containing 2 mM L-glutamine, 15 mM HEPES, 100 U/ml penicillin, 100 µg/ml Streptomycin (all from Sigma-Aldrich, Helsinki, Finland), B27 supplement (Gibco), 20 ng/

0959-4965 Copyright © 2019 The Author(s). Published by Wolters Kluwer Health, Inc. DOI: 10.1097/WNR.0000000000001372

ml epidermal growth factor (EGF; PeproTech EC Ltd, London, UK) and 10 ng/ml basic fibroblast growth factor (bFGF, PeproTech EC Ltd) and maintained in a humidified 5% CO_2/95% air incubator at 37°C. Within 3–5 days, the cells grew as free-floating neurospheres and were passaged after mechanical dissociation.

Materials

2′,7′-bis(carboxyethyl)-5,6-carboxyfluorescein acetoxymethyl ester (BCECF-AM) and bis-(1,3-dibutylbarbituric acid) trimethine oxonol ($DiBAC_4(3)$), were from Invitrogen, Life Technologies (Molecular Probes). All other chemicals used in the study were purchased from Sigma-Aldrich.

Solutions

The HEPES buffered medium (HBM) consisted of (in mM): 137 NaCl, 5 KCl, 2 $CaCl_2$, 0.44 KH_2PO_4, 4.2 $NaHCO_3$, 10 glucose, 10 HEPES and 0.5 $MgCl_2$. The pH was adjusted to 7.35 with NaOH. Low K^+ medium contained 0.44 KH_2PO_4 (medium from which the KCL had been omitted). All experiments were performed at 37°C under normal atmospheric conditions (21% O_2, 0.038% CO_2 in air).

Measurement of intracellular pH

Intracellular pH was measured in NPCs cell migrating outside the neurosphere using the cell-permeable probe BCECF-AM and a dual-wavelength InCytIm2 fluorescence imaging system (Intracellular Imaging Inc., Cincinnati, Ohio, USA) [25]. Cells differentiated for 3 days on poly-ornithine coated 25 mm round coverslips were loaded with 4 μM BCECF-AM in HBM for 12 minutes at 37°C. The cells were then washed three times with HBM, placed in the measuring chamber and transferred to a temperature-controlled chamber holder on the microscope (Nikon, TMS, 20× objective). During the experiment, the cells were superfused (1 ml/min) with warm (37°C) HBM pH 7.35. The cells were excited alternately with 490 and 440 wavelength light for 80 ms (rate of data capture 37 ratios/min). Images from 100 single cells were analyzed with the Incyt 4.5 software and further processed with Origin 6.0 (OriginLab Corp., Northampton, Massachusetts, USA) software. The BCECF fluorescence ratios of the 510 nm fluorescence were converted to pH values by using a standard curve [26]. Briefly, single cells located outside the neurosphere body were equilibrated in K^+ medium (140 mM) of varying pH (5.0–8.5) in the presence of 5 μM nigericin and calibration curves were constructed by plotting the extracellular pH against the corresponding fluorescence ratio. A sigmoidal relationship between the 490/440-nm fluorescence ratio and pH was observed between pH 6.0 and 8.0.

Measurement of membrane potential

Changes in the resting membrane potential of murine NPCs differentiated for 3 days were monitored using the potentiometric bisoxonol dye bis-(1,3-dibutylbarbituric acid)trimethine oxonol ($DiBAC_4(3)$), an anionic probe that, exhibits enhanced fluorescence when the cell membrane is depolarized (increased intracellular fluorescence due to dye influx). Conversely, hyperpolarization of the membrane potential leads to efflux of the probe and a decrease in fluorescence intensity. Cells cultured on 25 mm round coverslips were washed three times with HBM pH 7.35, placed in the measuring chamber and transferred to a temperature-controlled chamber holder on the microscope (Nikon, Diaphot 200 inverted microscope, 20× objective). For the experiment, 500 nM $DiBAC_4(3)$ was added to the perfusion solution (HBM pH 7.35) and allowed to equilibrate across the cell membrane for 15 minutes (1 ml/min) before the data acquisition process was started. The cells were excited with 470 nm wavelength light for 80 ms (rate of data capture 30/min) and the emitted fluorescence captured at 530 nm. The data were collected and analyzed with the Till Vision software and further processed with Origin 6.0 (OriginLab Corp.) software. At the end of each experiment, the cells were treated with depolarizing (20, 40 or 140 mM) K^+-solutions containing 500 nM $DiBAC_4(3)$ and the fluorescence signal was monitored. Membrane potential (E) was calculated using the Nernst equation assuming an intracellular potassium concentration of 140 mM and a temperature of 37°C. $E = 2.303 \times RT/zF \times \log10 ([K+]_e/[K+]_i)$.

Neurosphere formation assay

NSCs spheres were dissociated by vigorous pipetting using a Pasteur pipette, centrifuged and re-cultured in DMEM/F-12 'complete' culture medium (Gibco) containing 2 mM L-glutamine, 15 mM HEPES, 100 U/ml penicillin, 100 μg/ml Streptomycin (all from Sigma-Aldrich), B27 supplement (Gibco), 20 ng/ml EGF (PeproTech EC Ltd) and 10 ng/ml bFGF (PeproTech EC Ltd), and maintained in a humidified 5% CO_2/95% air incubator at 37°C. For the assay, suspensions of single cells were plated in 24-well plates (2 ml/well) and incubated for 3 days. Neurospheres formed in the cultures were visualized and photographed by using an Axiovert 135 inverted microscope equipped with a Zeiss AxioCam HRm digital camera. The diameter of the neurospheres formed in the culture (indicative of proliferation potential) was measured by using the ImageG software.

Neuronal differentiation

For neuronal differentiation neurospheres were plated on poly-DL-ornithine (Sigma) coated glass 25 mm round cover slips in the absence of EGF and FGF. Growth factor withdrawal induced spontaneous neuronal differentiation. The differentiated NPCs selected for pH and membrane potential measurements were single cells migrating towards the periphery, outside the neurosphere body. In the cell differentiation experiments, cells were allowed to differentiate for 3 days. Images were taken by using an Axiovert 135 inverted microscope equipped with a Zeiss AxioCam HRm digital camera (40× objective).

Statistics

Data are presented as means ± SEM (n = number of cells, N = number of independent experiments). In each experiment, 100 individual cells located from the neurosphere body edge to the outer edge of the culture were randomly chosen. Each experimental condition was repeated at least three times with independent NPC preparations. In all experiments, pH_i was allowed to decline for 4 minutes followed by calcium removal to initiate the pH recovery phase. Student's unpaired *t*-test was used to compare differences between the two cell populations.

Results

Effect of tannic acid on low potassium induced hyperpolarization and repolarization after calcium removal

In a previous study, we used low extracellular potassium (K^+ 0.44 mM) to trigger changes in the membrane potential in differentiated neural stem cells [23]. We found that, lowering extracellular potassium in the presence of 2 mM extracellular calcium-induced a prompt hyperpolarization (10–15 mV/min) in the whole cell population. A typical cell response in two cells that were hyperpolarized by superfusion with low extracellular K^+ (0.44 mM) is shown in Fig. 1a and b. These cells, which are radial glial-like cells, were located in the inner area close to the neurosphere edge. In control cells, removal of extracellular calcium-induced a rapid depolarization of the membrane potential (Fig. 1a). In our hands, this depolarization is dependent on extracellular Na^+ since it does not occur in medium where all Na^+ is replaced with N-methyl-D-glucamine (data not shown). However, in the presence of 100 µM TA, the depolarization process was inhibited (Fig. 1b). Washout of TA triggered depolarization in a fraction of the cell population (Table 1).

Fig. 1

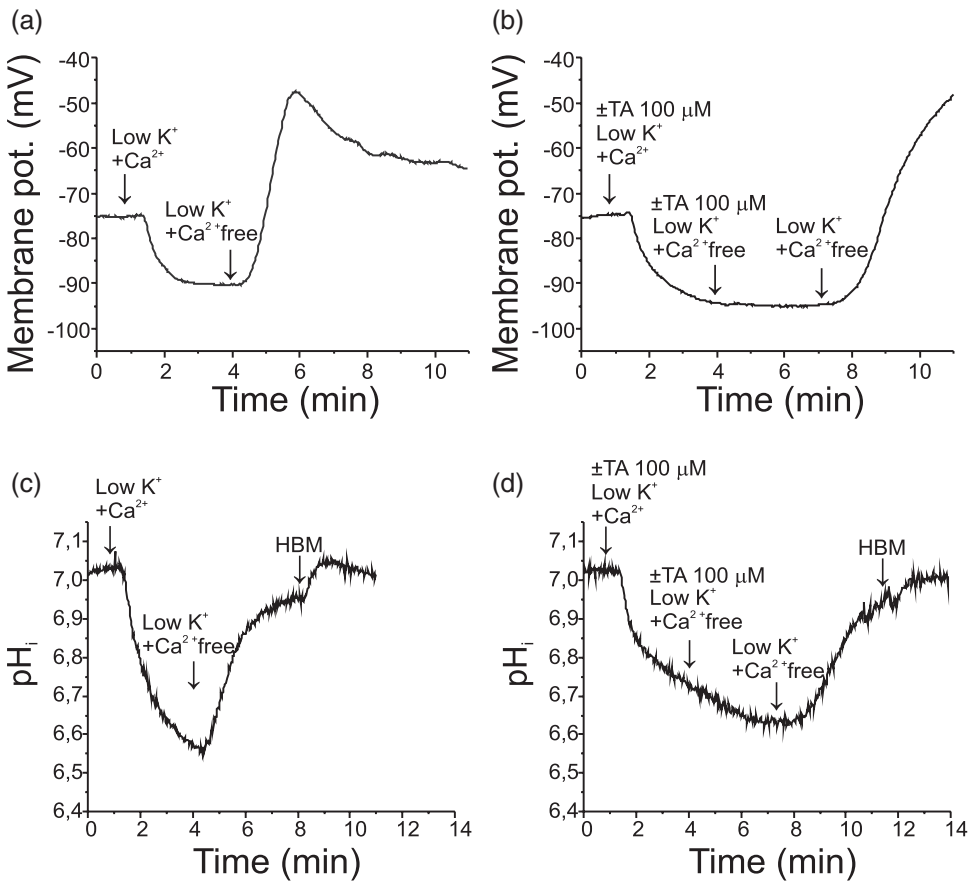

Change in membrane potential and pH_i in stem cell-derived radial glial-like cells upon exposure to low extracellular K^+ in the presence or absence of TA. (a) Low 0.44 mM K^+ induced a hyperpolarization while a prompt depolarization occurred after removal of extracellular calcium. (b) In the presence of 100 µM TA, the depolarization induced by calcium removal was inhibited. Washout of TA after 7 minutes perfusion allowed depolarization in a fraction of the cells. (c) Intracellular pH response in inner radial-glial like cells exposed to low extracellular K^+ (0.44 mM K^+) in the presence of 2 mM extracellular calcium. After 4 minutes of superfusion, extracellular calcium was removed. (d) In the experiment where TA was present, TA free perfusion with Ca^{2+} free medium containing 0.44 mM K^+ was started at 7 minutes. In each individual experiment, membrane potential and pH responses from 100 cells were recorded. Representative traces are shown. Statistics of these experiments (three independent experiments) are shown in Table 1. TA, tannic acid.

Tannic acid affects NBCe1 mediated pHi regulation in glial-like progenitor cells

We have previously shown that NBCe1 mediated pHi regulation can be studied in stem cell-derived radial glial-like cells by manipulating the extracellular K^+ concentration [23]. When this cell population is exposed to low extracellular K^+, an intracellular acidification takes place due to electrogenic HCO_3^- extrusion, whereas H^+ ions are left behind (Fig. 1c).

However, if extracellular calcium is removed, a rapid sodium-dependent depolarization takes place which in turn induces a rapid pH_i recovery due to HCO_3^- influx via the electrogenic Na^+/HCO_3^- cotransporter NBCe1 (Slc4a4) [23] ($1Na^+/2HCO_3^-$ stoichiometry) (Fig. 1c). As shown in Fig. 1d, 100 μM TA slowed down the acidification process and completely inhibited the pH recovery process after calcium removal. However, rapid washout of the TA allowed pH recovery in a fraction of the cells (Fig. 1d and Table 1).

Table 1 Effects of TA on membrane potential and cytosolic pH

Parameter	Control cells	TA 100 μM
Effects of tannic acid on membrane potential		
Low K^+ induced membr. pot. change (mV)	−15.23 ± 0.65	−17.86 ± 2.12
Cells hyperpolarized (% of all cells)	100	100
Cells depolarized after Ca^{2+} removal (%)	28.0 ± 1.29	2.77 ± 0.80[a]
Cells depolarized after TA washout (%)		7.20 ± 3.75
Effects of TA on cytosolic pH		
Low K^+ induced pH_i change	−0.48 ± 0.65	−0.36 ± 0.02
Cells acidified (%)	36.97 ± 2.59	22.83 ± 2.4
pH_i recovery after Ca^{2+} removal (%)	18.88 ± 1.57	1.66 ± 1.20[a]
pH_i recovery after TA washout (%)		8.73 ± 2.70

Values are means ± SEM calculated on the whole cell population; n = 3, N = 100 cells in each experiment.
TA, tannic acid.
[a]$P < 0.005$ vs. control (Student *t*-test).

Tannic acid inhibits neural stem cell proliferation and neurosphere formation

To study the effects of TA on neural stem cell proliferation, a single cell suspension of neural stem cells was incubated in the presence of various concentrations of TA. As shown in Fig. 2c, 50 μM TA induced a complete block of neural stem cell proliferation (neurosphere formation) while neurospheres could be formed in the cultures treated with 25 μM TA (Fig. 2d). The average neurosphere diameter in the cultures treated with 25, 5 or 1 μM TA was 153.4 ± 4.2, 164.7 ± 4.3 and 181.1 ± 4.2 μM, respectively, compared to 180.2 ± 3.7 μM in control cultures. In cultures treated with 50 or 100 μM TA only single cells could be observed (Fig. 2b and c).

Tannic acid inhibits neural stem cell differentiation

Neural stem cell differentiation can be studied in a neural stem cell culture by placing neurospheres on poly-ornithine coated dishes in the absence of the growth factors EGF and FGF (differentiation medium). In the absence of growth factors progenitor cells generate neurons and radial glia cells through asymmetric division. Radial glia

Fig. 2

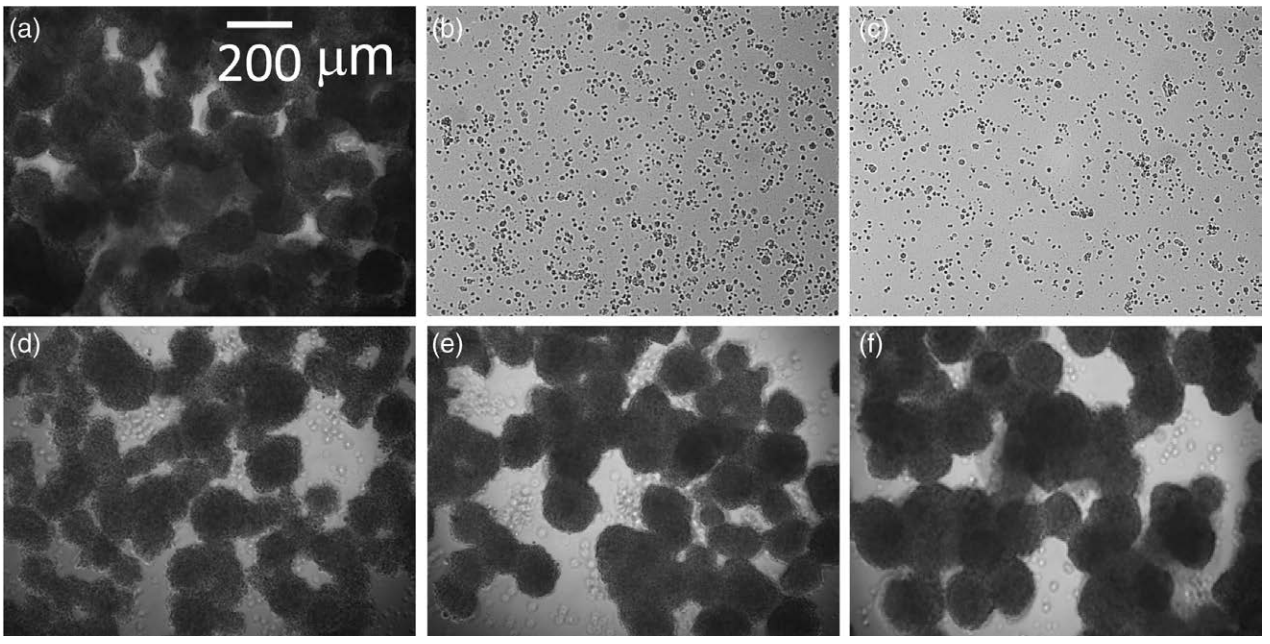

Inhibition of sodium/bicarbonate cotransporters (NBCs) with tannic acid affects neural stem cell proliferation. Images show neurospheres formed within 72 hours in control cell culture (a) and cells treated with 100 μM (b), 50 μM (c), 25 μM (d), 5 μM (e) and 1 μM TA (f). Representative images (10× objective) from one experiment are shown. The experiment was repeated three times with similar results.

cells form a network of radial processes that support neuronal migration and axon guidance. A typical cell differentiation pattern with an inner cell layer consisting of radial glial-like cells and an outer layer with radial glia cells and migrating neurons is shown in Fig. 3a. The presence of 5 μM TA, almost completely inhibited the formation of the glial layer and neurons and dead cells were found outside the neurospheres (Fig. 3c). However, treatment of neurospheres with 5 μM (Fig. 3e) or 25 μM TA (Fig. 3f) for 24 hours, followed by a washing step and re-culturing for 48 hours, resulted in cell differentiation in both cultures.

Discussion

We have recently shown that the dominating pH_i regulating system in stem cell-derived radial glial-like cells is the electrogenic sodium bicarbonate co-transporter NBCe1 (Slc4a4) [23]. We reported that neural stem cell differentiation and proliferation could be inhibited by S0859, a potent NBCe1 inhibitor. To our knowledge, a natural inhibitor for NBCe1 has not yet been described.

Since, TA, a natural antioxidant, has previously been shown to affect various intracellular signaling systems, including cell proliferation and progression through the cell cycle, we here looked at its effects on pH_i regulation.

Fig. 3

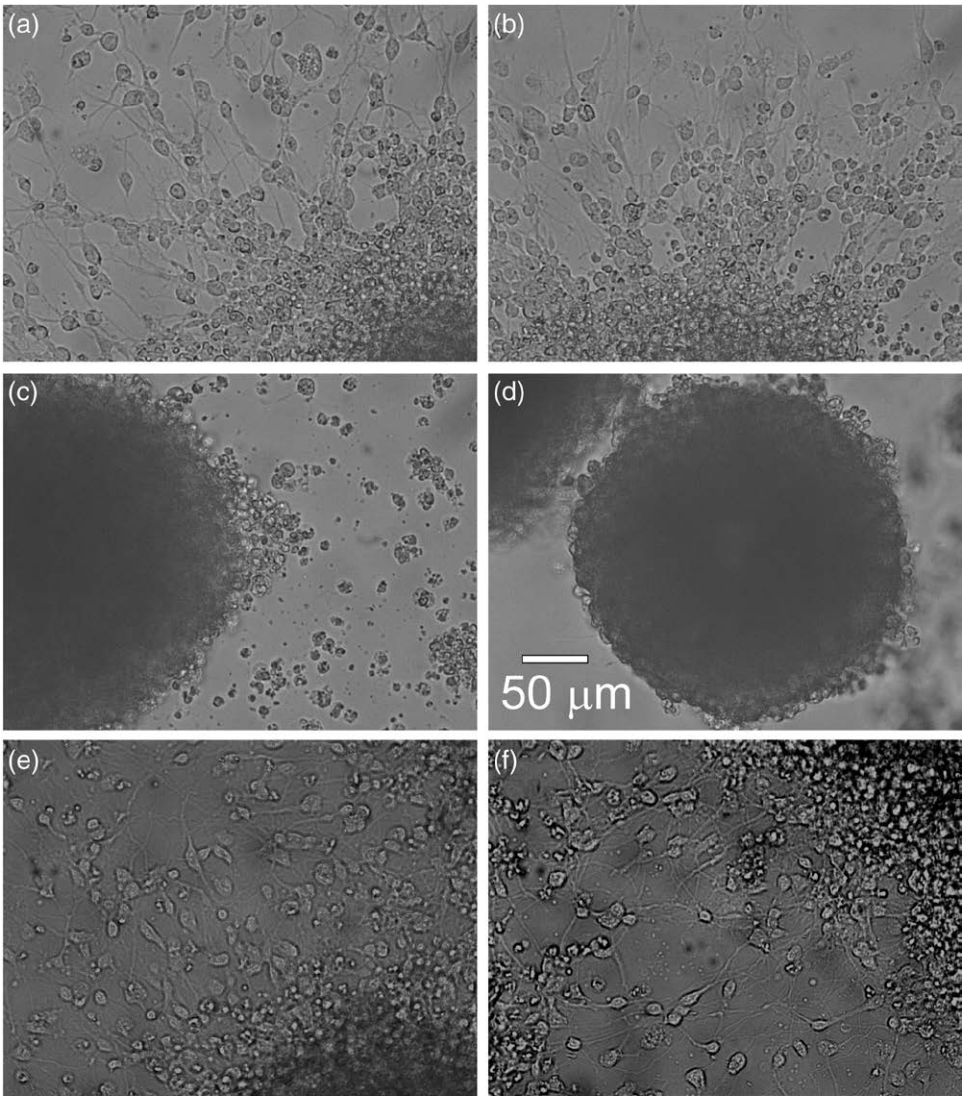

Inhibition of Na^+/HCO_3^- cotransporter activity by tannic acid (TA) affects neural stem cell differentiation. Images show radial glia cells and migrating neurons formed within 72 hours after growth factors removal in control cell culture (a) and cells treated with 1 μM (b), 5 μM (c) and 25 μM (d) TA. Cells treated with 5 μM (e) and 25 μM (f) TA for 24 hours, washed and re-cultured for 48 hours in normal differentiation medium. A representative set of gray-scale images (40× objective) from one experiment out of three conducted are shown.

Here we show for the first time, that TA can interfere with a critical pH_i regulating system in radial glial-like cells by blocking the NBCe1 activity. The block was evident in glial-like cells that had been acidified by low K^+ induced hyperpolarization. The rapid depolarization that took place in hyperpolarized cells after removal of extracellular calcium was efficiently blocked by TA. Our data indicate that during our experimental conditions, TA induced block on NBCe1 is either on a calcium-regulated Na^+ channel that is responsible for the depolarization or due to a direct effect on the NBCe. We think that the effect observed is directly on the NBCe1 since addition of 20 mM extracellular K^+ in the presence of 100 µM TA to cells acidified with low extracellular potassium, triggered a rapid depolarization (19.5 ± 1.6 mV/min) but a very modest pH_i recovery (0.005 pH/min as compared to 0.2 ± 0.03 pH/min in control cells). Washout of TA allowed pH_i recovery to control levels (recovery rate 0.04 pH/min).

In addition to interfering with Na^+-dependent membrane potential changes and pH_i regulation, we found that neural stem cell differentiation and the formation of radial glial cells and migrating neurons, were strongly inhibited by the presence of TA. A concentration of 5 µM already affected the cell differentiation process. Higher concentrations of TA completely blocked neurosphere formation from single cells and the formation of progenitor cells that are responsible for radial glia and neuron formation. TA did not induce acute cytotoxicity to the glial progenitor cell population since the TA inhibition of the cell differentiation process could be reversed if the cultures were washed after 24 hours treatment.

Previous data strongly indicate that rapid alterations in both membrane potential and intracellular pH take place during critical steps during the cell cycle [27]. In particular, transition from G0/G1 into S phase seems to involve changes in membrane potential [28,29]. We found that TA treatment prevented rapid alterations in both membrane potential and intracellular pH. We believe that these effects on pH_i regulation and membrane potential affected progenitor stem cell progression through the cell cycle. Most importantly, TA or compounds with similar NBCe1 inhibiting properties might be valuable tools to sensitize glioma stem cells within high-grade glioma to chemotherapeutics such as Temozolomide [30].

Acknowledgements

We are grateful for the laboratory assistance provided by Jarno Hörhä.

Supported by grants from the K. Albin Johansson foundation and the Magnus Ehrnrooth Foundation.

Conflicts of interest

There are no conflicts of interest.

References

1 Chung KT, Wong TY, Wei CI, Huang YW, Lin Y. Tannins and human health: a review. *Crit Rev Food Sci Nutr* 1998; **38**:421–464.
2 Andrade RG Jr, Dalvi LT, Silva JM Jr, Lopes GK, Alonso A, Hermes-Lima M. The antioxidant effect of tannic acid on the *in vitro* copper-mediated formation of free radicals. *Arch Biochem Biophys* 2005; **437**:1–9.
3 Andrade RG Jr, Ginani JS, Lopes GK, Dutra F, Alonso A, Hermes-Lima M. Tannic acid inhibits *in vitro* iron-dependent free radical formation. *Biochimie* 2006; **88**:1287–1296.
4 Lopes GK, Schulman HM, Hermes-Lima M. Polyphenol tannic acid inhibits hydroxyl radical formation from Fenton reaction by complexing ferrous ions. *Biochim Biophys Acta* 1999; **1472**:142–152.
5 Karakurt S, Adali O. Tannic acid inhibits proliferation, migration, invasion of prostate cancer and modulates drug metabolizing and antioxidant enzymes. *Anticancer Agents Med Chem* 2016; **16**:781–789.
6 Yang P, Ding GB, Liu W, Fu R, Sajid A, Li Z. Tannic acid directly targets pyruvate kinase isoenzyme M2 to attenuate colon cancer cell proliferation. *Food Funct* 2018; **9**:5547–5559.
7 Darvin P, Joung YH, Kang DY, Sp N, Byun HJ, Hwang TS, *et al*. Tannic acid inhibits EGFR/STAT1/3 and enhances p38/STAT1 signalling axis in breast cancer cells. *J Cell Mol Med* 2017; **21**:720–734.
8 Nagesh PKB, Hatami E, Chowdhury P, Kashyap VK, Khan S, Hafeez BB, **et al**. Tannic acid induces endoplasmic reticulum stress-mediated apoptosis in prostate cancer. *Cancers (Basel)* 2018; **10**:E68.
9 Zhang J, Chen D, Han DM, Cheng YH, Dai C, Wu XJ, **et al**. Tannic acid mediated induction of apoptosis in human glioma hs 683 cells. *Oncol Lett* 2018; **15**:6845–6850.
10 Zielińska-Przyjemska M, Kaczmarek M, Krajka-Kuźniak V, Łuczak M, Baer-Dubowska W. The effect of resveratrol, its naturally occurring derivatives and tannic acid on the induction of cell cycle arrest and apoptosis in rat C6 and human T98G glioma cell lines. *Toxicol in Vitro* 2017; **43**:69–75.
11 Sen HM, Ozkan A, Guven M, Akman T, Aras AB, Sehitoglu I, **et al**. Effects of tannic acid on the ischemic brain tissue of rats. *Inflammation* 2015; **38**:1624–1630.
12 Winiarska-Mieczan A. Protective effect of tannic acid on the brain of adult rats exposed to cadmium and lead. *Environ Toxicol Pharmacol* 2013; **36**:9–18.
13 Nam S, Smith DM, Dou QP. Tannic acid potently inhibits tumor cell proteasome activity, increases p27 and Bax expression, and induces G1 arrest and apoptosis. *Cancer Epidemiol Biomarkers Prev* 2001; **10**:1083–1088.
14 Yang EB, Wei L, Zhang K, Chen YZ, Chen WN. Tannic acid, a potent inhibitor of epidermal growth factor receptor tyrosine kinase. *J Biochem* 2006; **139**:495–502.
15 Darvin P, Baeg SJ, Joung YH, Sp N, Kang DY, Byun HJ, **et al**. Tannic acid inhibits the jak2/STAT3 pathway and induces G1/S arrest and mitochondrial apoptosis in YD-38 gingival cancer cells. *Int J Oncol* 2015; **47**:1111–1120.
16 Song D, Zhao J, Deng W, Liao Y, Hong X, Hou J. Tannic acid inhibits NLRP3 inflammasome-mediated IL-1β production via blocking NF-κb signaling in macrophages. *Biochem Biophys Res Commun* 2018; **503**:3078–3085.
17 Szteyn K, Schmid E, Nurbaeva MK, Yang W, Münzer P, Kunzelmann K, **et al**. Expression and functional significance of the ca(2+)-activated cl(-) channel ANO6 in dendritic cells. *Cell Physiol Biochem* 2012; **30**:1319–1332.
18 Namkung W, Thiagarajah JR, Phuan PW, Verkman AS. Inhibition of ca2+-activated cl- channels by gallotannins as a possible molecular basis for health benefits of red wine and green tea. *Faseb J* 2010; **24**:4178–4186.
19 Gallos G, Remy KE, Danielsson J, Funayama H, Fu XW, Chang HY, **et al**. Functional expression of the TMEM16 family of calcium-activated chloride channels in airway smooth muscle. *Am J Physiol Lung Cell Mol Physiol* 2013; **305**:L625–L634.
20 Chu X, Guo Y, Xu B, Li W, Lin Y, Sun X, **et al**. Effects of tannic acid, green tea and red wine on herg channels expressed in HEK293 cells. *Plos One* 2015; **10**:e0143797.
21 Zhang Y, Chu X, Liu L, Zhang N, Guo H, Yang F, **et al**. Tannic acid activates the kv7.4 and kv7.3/7.5 K(+) channels expressed in HEK293 cells and reduces tension in the rat mesenteric arteries. *J Pharm Pharmacol* 2016; **68**:494–502.
22 Zhu F, Chu X, Wang H, Zhang X, Zhang Y, Liu Z, **et al**. New findings on the effects of tannic acid: inhibition of L-type calcium channels, calcium transient and contractility in rat ventricular myocytes. *Phytother Res* 2016; **30**:510–516.
23 Nordström T, Andersson LC, Åkerman KEO. Regulation of intracellular ph by electrogenic na+/HCO3- co-transporters in embryonic neural stem

cell-derived radial glia-like cells. *Biochim Biophys Acta Biomembr* 2019; **1861**:1037–1048.
24 Kärkkäinen V, Louhivuori V, Castrén ML, Akerman KE. Neurotransmitter responsiveness during early maturation of neural progenitor cells. *Differentiation* 2009; **77**:188–198.
25 Nordström T, Jansson LC, Louhivuori LM, Akerman KE. Effects of acute hypoxia/acidosis on intracellular ph in differentiating neural progenitor cells. *Brain Res* 2012; **1461**:10–23.
26 Nordström T, Rotstein OD, Romanek R, Asotra S, Heersche JN, Manolson MF, **et al**. Regulation of cytoplasmic ph in osteoclasts. Contribution of proton pumps and a proton-selective conductance. *J Biol Chem* 1995; **270**:2203–2212.
27 Blackiston DJ, McLaughlin KA, Levin M. Bioelectric controls of cell proliferation: ion channels, membrane voltage and the cell cycle. *Cell Cycle* 2009; **8**:3527–3536.
28 Wonderlin WF, Woodfork KA, Strobl JS. Changes in membrane potential during the progression of MCF-7 human mammary tumor cells through the cell cycle. *J Cell Physiol* 1995; **165**:177–185.
29 Sundelacruz S, Levin M, Kaplan DL. Role of membrane potential in the regulation of cell proliferation and differentiation. *Stem Cell Rev Rep* 2009; **5**:231–246.
30 Stéphanou A, Ballesta A. Ph as a potential therapeutic target to improve temozolomide antitumor efficacy: a mechanistic modeling study. *Pharmacol Res Perspect* 2019; **7**:e00454.